On the Rapid Synthesis of Reduced Graphene Oxide via Ultrasound-Promoted Eco-Friendly Reduction Approach and Its Effects on Physicochemical Properties

Shuen Lam[1], Fei Wang[1], Swee Pin Yeap[1,2,*], Kah Hou Teng[2,3,*], Andy Shaw[4], Vijayakumar Karunamoothei[4], Vahid Khosravi[1,2], Chengyi Liu[5,*]

[1] Department of Chemical & Petroleum Engineering, Faculty of Engineering, Technology & Built Environment, UCSI University, 56000, Cheras, Kuala Lumpur, Malaysia
[2] UCSI-Cheras Low Carbon Innovation Hub Research Consortium, Kuala Lumpur, Malaysia.
[3] Department of Mechanical and Mechatronics Engineering, Faculty of Engineering, Technology and Built Environment, UCSI University, 56000, Kuala Lumpur, Malaysia
[4] Built Environment and Sustainable Technologies (BEST) Research Institute, Liverpool John Moores University, United Kingdom
[5] School of Electronic and Information Engineering, Changshu Institute of Technology, Suzhou 215500, China

*Corresponding author: yeapsw@ucsiuniversity.edu.my; tengkh@ucsiuniversity.edu.my; chengyiliu@cslg.edu.cn

Abstract

The common synthesis approach of reduced graphene oxide (rGO) using toxic reducing agents poses a threat to environmental pollution. This study used banana peel extract as a green reducing agent for the synthesis of rGO. Ultrasonication was assimilated to expedite the synthesis process. For comparison, rGO was also produced by reducing GO with hydrazine treatment under conventional stirring. Both morphological (SEM) and physicochemical (FTIR and XRD) studies have revealed that banana peel extract can reduce GO to rGO, although its reducing effect is much weaker compared to hydrazine. Despite this, the rGO produced using banana peel extract with the assimilation of ultrasonication technique has a greater interlayer spacing than that formed under the conventional stirring method. In terms of electrical properties, the electrical conductance of hydrazine-produced rGO (5.69 ×

10^{-6} S) is higher than the banana peel extract-produced rGO (3.55×10^{-6} S - 4.56×10^{-6} S). Interestingly, it was found that most of the rGO produced by banana peel extract under ultrasound assistance has higher or comparable electrical conductance compared to the rGO produced by banana peel extract under stirring method. This implies the feasibility of using short-period ultrasound to replace conventional stirring in rGO synthesis.

1. Introduction

Since its discovery in 2004, graphene nanomaterials have been at the center of focus in many applications, and numerous breakthroughs have been made in their synthesis and applications [1]. Graphene oxide (GO) is a single-layer sheet formed by oxidation of graphite with oxygen-containing functionalities. GO nanoparticles have been widely used recently particularly for environmental treatment [2]. In the synthesis of GO, disruption of the sp^2 bonding orbitals and addition of oxygen-containing surface groups lead to a reduction in the electrical conductivity [3]. Due to this, researchers have investigated GO reduction techniques to produce reduced graphene oxide (rGO) which can considerably restore its electrical conductivity ranging from 0.1 S m^{-1} to 2.98×10^4 S m^{-1} [3a]. With the presence of electrical conductivity, rGO may contribute to the production of composites to enhance the performance of supercapacitor and flexible sensor [4].

There are several approaches to reduce GO to rGO which include thermal treatment, electrochemical reduction, and chemical reagents. Among these approaches, the method using chemical reagents is still considered to have the highest effectiveness for rGO production. Unlike for thermal treatment, the chemical method requires a lower amount of energy and simpler set-up, whereas the electrochemical reduction has a lower efficiency compared to the conventional method [5]. In the chemical reduction process, several reducing

agents are currently in use to efficiently reduce GO, such as hydrazine, sodium borohydride ($NaBH_4$) and strong alkaline solutions. These types of reducing agents are not environmentally friendly, thus making them less suitable for utilization in large-scale production [6]. Hence, there is a practical need to reduce the environmental impact caused by the usage of hazardous reducing agents/chemicals by replacing them with an environmentally friendly alternative [7].

Currently, researchers are exploring safer, eco-friendly, and green synthesis pathways for GO reduction. This can be done by using natural compounds such as juice extracts [8], fruit peels extract [6], plant extract [9], and tea extract [10] as reducing agents. The abundance of reducing species in the extracts, particularly polyphenols, can attack the sp2 carbon atom at the GO's epoxide ring lead to the formation of C–O–C bond between GO and polyphenol; as the reaction proceeds, other C–O–C bonds yield the desired rGO [11]. However, the reduction duration for GO in most studies is relatively lengthy under conventional stirring; notably, the process may extend from a few hours up to 48 hours. Therefore, another potential research topic in this area is to expedite the reduction process.

Due to the unique impact of the intense reaction conditions which include high temperature and pressure occurring inside the continually collapsed and formed cavities, sonochemistry is receiving a lot of attention recently for the purpose of expediting mixing and reaction rate [12]. A recent study by Vartolomei demonstrated that the efficiency of the esterification reaction could be enhanced with a shorter reaction time by incorporating ultrasonication [13]. In fact, sonication has been used as a crucial step to exfoliate graphene sheets from graphite [14]. Through this, it is envisaged that the reaction time can be reduced drastically with sonication to achieve a rapid and facile synthesis of rGO. In consideration of

the importance of minimizing environmental impact and shortening synthesis time, this project aimed to evaluate feasibility of synthesizing rGO using an ultrasound-promoted green reduction method. This method utilizes banana peel extract as the environmentally friendly reducing agent, while adjusting ultrasound amplitude and duration. Banana peel was chosen because it is rich in antioxidant and antibacterial compounds including phenolic compounds, alkaloids, flavonoids, tannins, catecholamines (dopamine), vitamin C, etc that can serve as reducing agent [15]. The antioxidant properties of banana peel extracts have been proven in numerous past studies through DPPH (2,2-diphenyl-1-picrylhydrazyl) and ABTS (2,2-azinobis (3-ethylbenzthiazo-line-6-sulphonic acid) radical scavenging assays [15c, 16].

2. Results and Discussion

Visual Observation on Synthesized Nanoparticles

Visual Observation on GO Synthesis

In this study, GO was synthesized via the modified Hummers' method. Figure 1a shows the well-dispersed GO suspension that appeared in a brownish-yellow color [17]. The dispersibility was rather high due to the hydrophilic nature of this nanoparticle. Meanwhile, the GO paste and the dried GO flakes appeared black, as illustrated in Figures 1b and 1c.

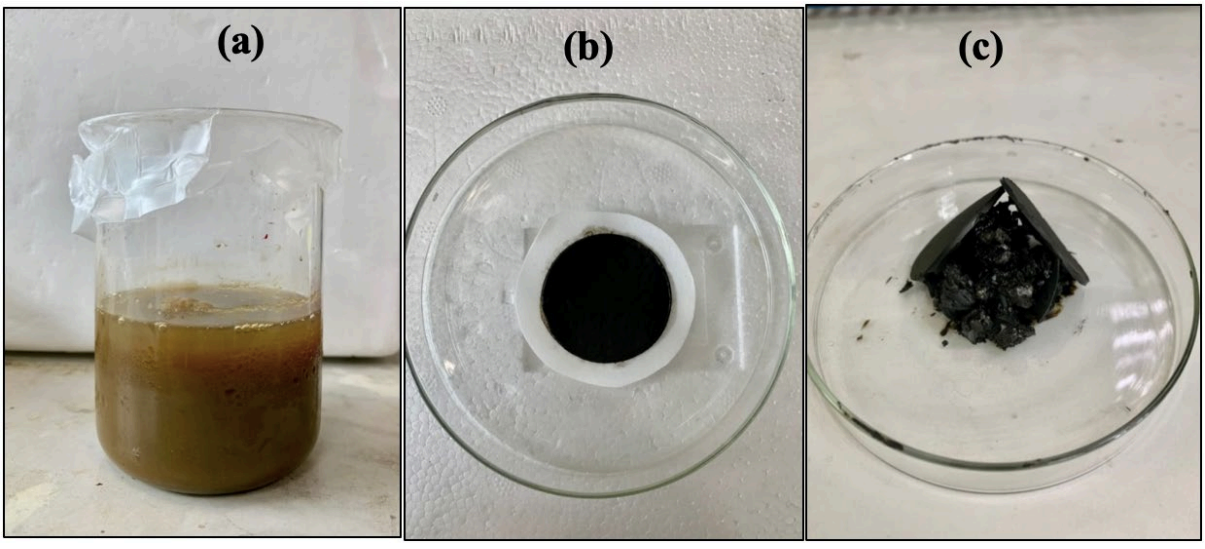

Figure 1. Digital images of (a) GO suspension, (b) GO paste, and (c) dried GO flakes.

Visual Observation on rGO Synthesis

The rGO was synthesized via a reduction process by using banana peel extract and hydrazine hydrate as the reducing agents. As shown in Figure 2, the rGO reduced using banana peel extract and hydrazine hydrate under a 3-hour stirring condition appeared as dry black powder. It is noteworthy that the physical structure of rGO formed using banana peel extract is similar to those formed using hydrazine hydrate.

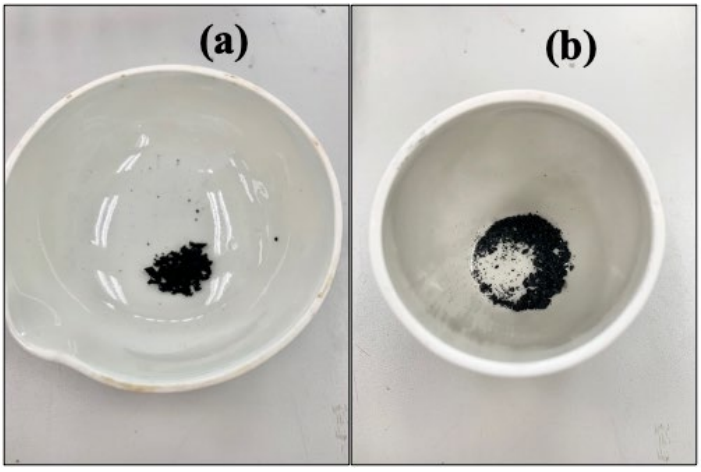

Figure 2. Digital images of rGO powder formed using (a) banana peel extract and (b) hydrazine hydrate reduction under a conventional 3-hour stirring method.

Next, the GO was reduced using banana peel extract with the assimilation of ultrasound technique. As shown in Figures 3a and 3b, the rGO produced via the ultrasonic approach was all in the form of black powder. Overall, the physical structure of rGO formed using banana peel extract (with the assimilation of ultrasound technique) is similar to that formed using the stirring method.

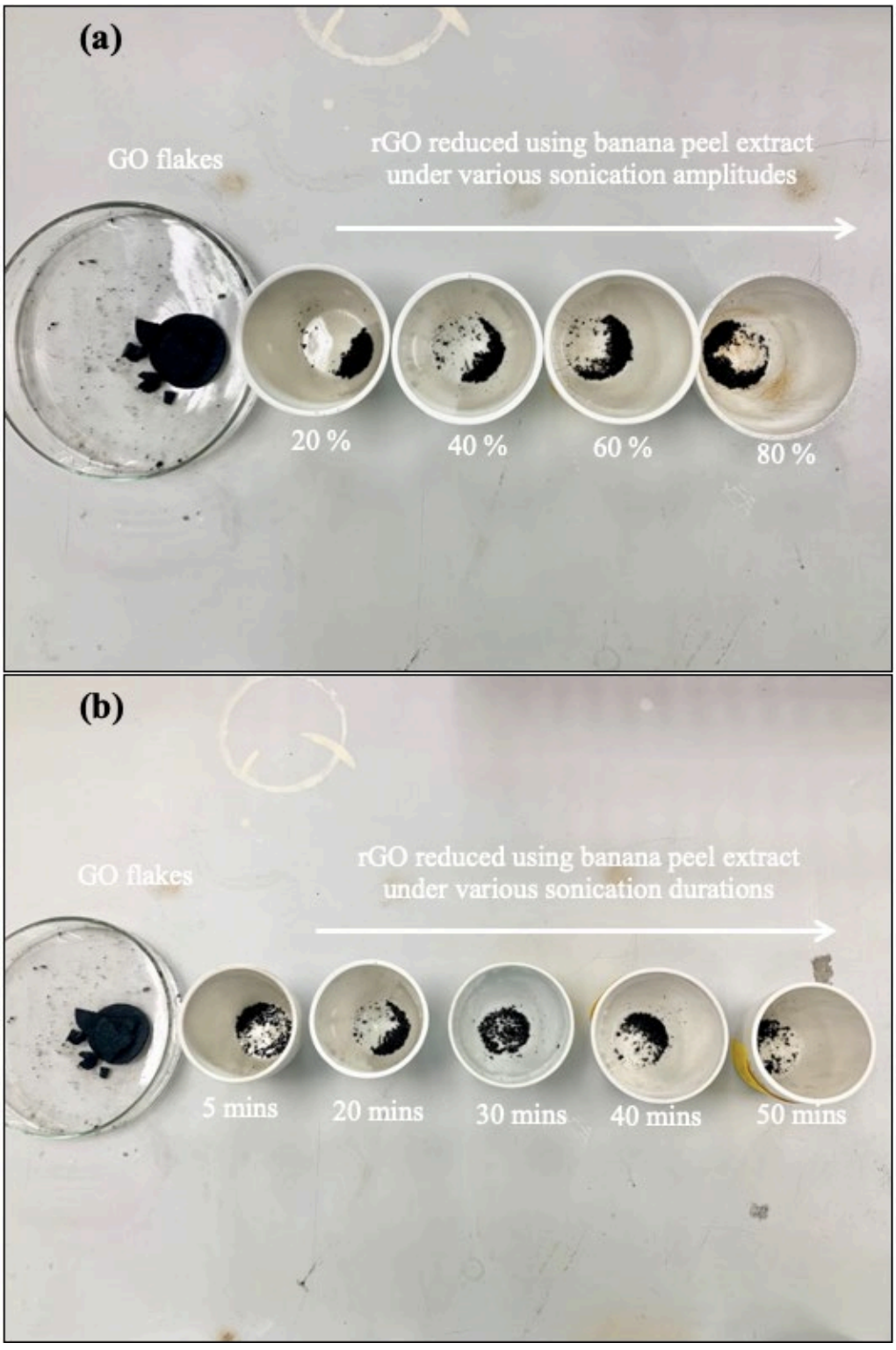

Figure 3. Digital images of GO flakes and rGO reduced using banana peel extract under various (a) sonication amplitudes of 20 %, 40 %, 60 % and 80 %, and (b) sonication durations of 5 mins, 20 mins, 30 mins, 40 mins, and 50 mins.

Morphological Analysis

SEM Analysis of Graphite and GO

Figure 4a shows that the purchased graphite particles have a flake shape with irregular sizes. The particles have rough surfaces with a multilayered (thick) structure. The closely stacked carbon layers can be observed due to strong van der Waals forces that attract the graphene layers together. On the other hand, the as-synthesized GO can be seen with a flaky texture with a folded and wrinkled structure (Figure 4b). In particular, the formation of oxygen-functional groups including hydroxyl and epoxy may alter the hybridization of sp^2 carbons (planar structure) to sp^3 carbons (tetrahedral structure), leading to the observed wrinkled morphology [18].

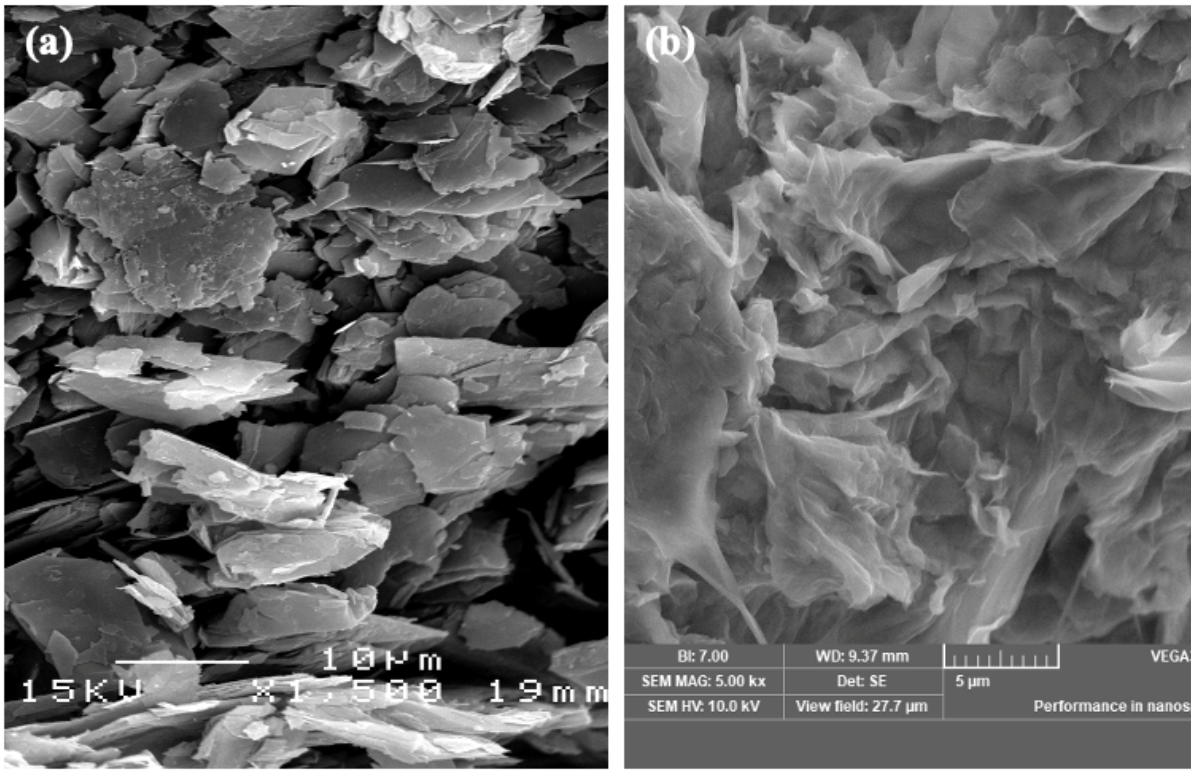

Figure 4. The SEM images of (a) graphite and (b) GO.

SEM Analysis of rGO Synthesized Based on Stirring Method

Figure 5 shows the SEM images of the rGO synthesized using hydrazine hydrate and banana peel extract under 3 hours of stirring. As depicted in Figure 5 (a.i) and (b.i), both rGO samples formed clusters with roughened surfaces. At higher magnification (5000x), it was observed that both rGOs consisted of layers of wavy, folded, and wrinkled surfaces which developed the sinuate structural properties. The rGO surfaces are corrugated owing to the removal of oxygen functional groups during the reduction process [19]. Overall, it was seen that rGO (Figure 5) has a more corrugated structure than GO (Figure 4b). Despite this, it is worth noting that the extent of corrugation is more pronounced for rGO produced via hydrazine hydrate reduction, preliminary suggesting that hydrazine hydrate is a more effective reducing agent compared to banana peel extract.

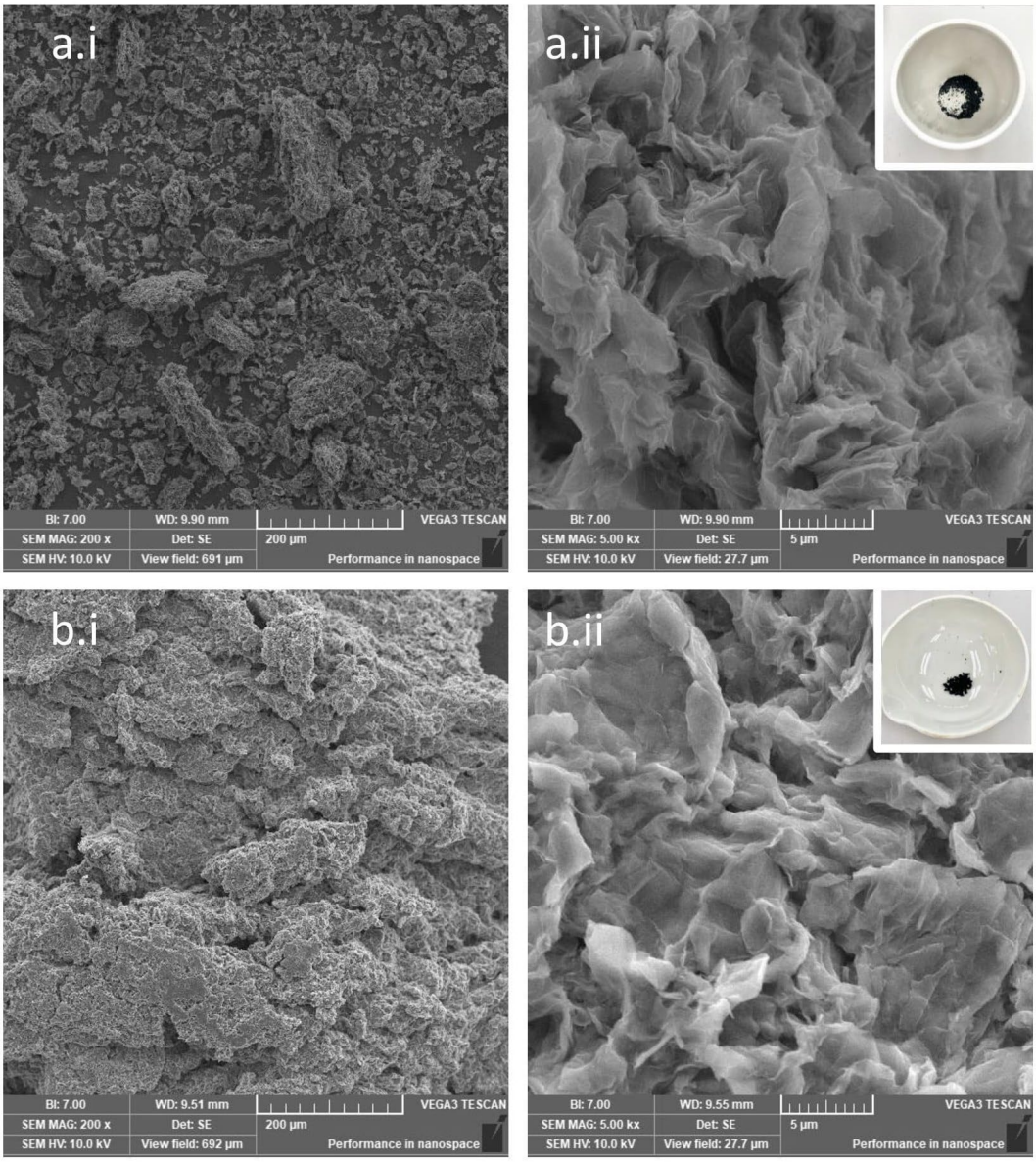

Figure 5. SEM images of rGO synthesized using (a) hydrazine hydrate and (b) banana peel extract under conventional 3 hours stirring method (*i.* 200x magnification and *ii.* 5000x magnification).

Interlayer spacing of rGO layers is one of the factors affecting the electrical conductivity of produced rGO [20]. Theoretically, GO exhibits a larger interlayer spacing compared to rGO due to the attached functional groups on its surface [21]. Conversely, a smaller interlayer spacing of rGO is due to the removal of functional groups on its surface during the reduction process [22]. In this study, the interlayer spacing of rGO layers was

determined to compare the quality of rGO synthesized using different reducing agents. As shown in Figure 6, the rGO produced using hydrazine hydrate and banana peel extract has an interlayer spacing of 0.77 μm and 0.63 μm, respectively. T-test analysis has shown the *p*-value to be above 0.05 for both samples, indicating that both samples are not significantly different. Therefore, the result suggests that banana peel extract is a potential substitute for hydrazine hydrate in synthesizing rGO with similar interlayer spacing.

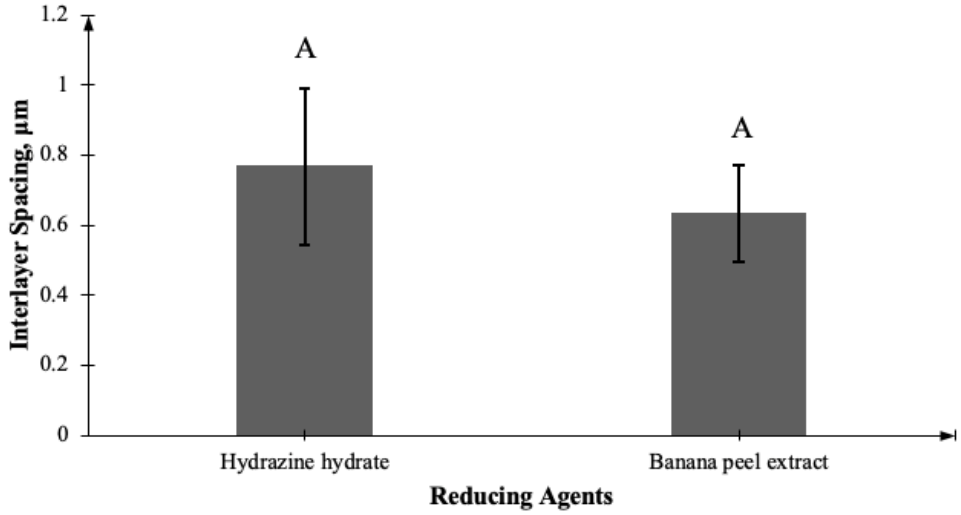

Figure 6. Interlayer spacing of rGO produced by the reduction process using various reducing agents under a conventional 3-hour stirring method (*Statistically significant study by t-test at $P < 0.05$).

SEM Analysis of rGO Synthesized Based on Various Sonication Conditions

Figure 7 shows the SEM images of rGO synthesized using banana peel extract under various sonication amplitudes. Overall, it was observed that all of the rGO exhibited rough and irregular surfaces. At a higher magnification (5000x), it was clearly seen that the rGO showed wavy and wrinkled layers stacking on top of one another in agglomerated forms, forming an overlapped 3D structure.

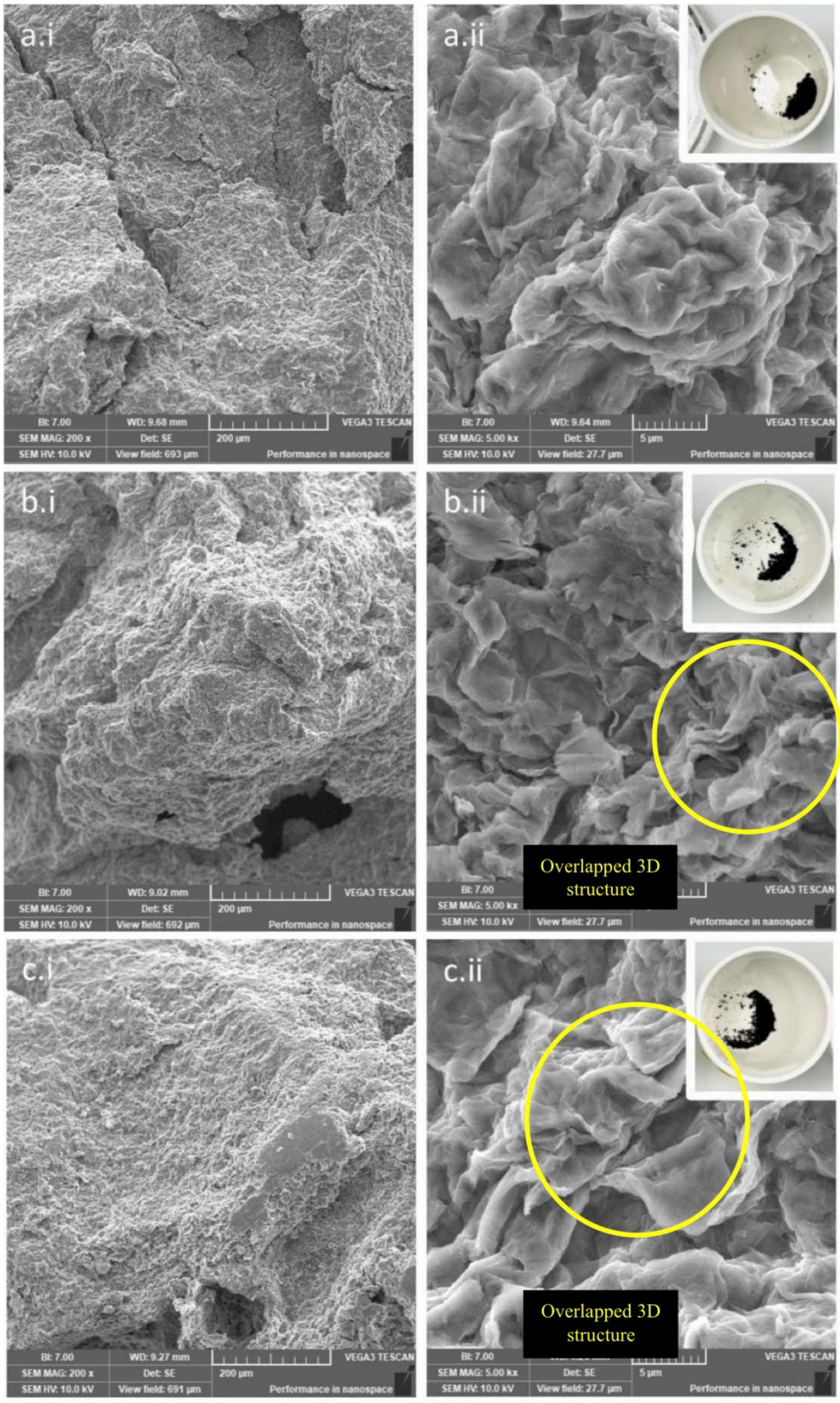
a.i
BI: 7.00
WD: 9.68 mm
VEGA3 TESCAN
SEM MAG: 200 x
Det: SE
200 µm
SEM HV: 10.0 kV
View field: 693 µm
Performance in nanospace
a.ii
BI: 7.00
WD: 9.64 mm
VEGA3 TESCAN
SEM MAG: 5.00 kx
Det: SE
5 µm
SEM HV: 10.0 kV
View field: 27.7 µm
Performance in nanospace
b.i
BI: 7.00
WD: 9.02 mm
VEGA3 TESCAN
SEM MAG: 200 x
Det: SE
200 µm
SEM HV: 10.0 kV
View field: 692 µm
Performance in nanospace
b.ii
Overlapped 3D structure
BI: 7.00
VEGA3 TESCAN
SEM MAG: 5.00 kx
SEM HV: 10.0 kV
View field: 27.7 µm
Performance in nanospace
c.i
BI: 7.00
WD: 9.27 mm
VEGA3 TESCAN
SEM MAG: 200 x
Det: SE
200 µm
SEM HV: 10.0 kV
View field: 691 µm
Performance in nanospace
c.ii
Overlapped 3D structure
BI: 7.00
VEGA3 TESCAN
SEM MAG: 5.00 kx
Det: SE
5 µm
SEM HV: 10.0 kV
View field: 27.7 µm
Performance in nanospace

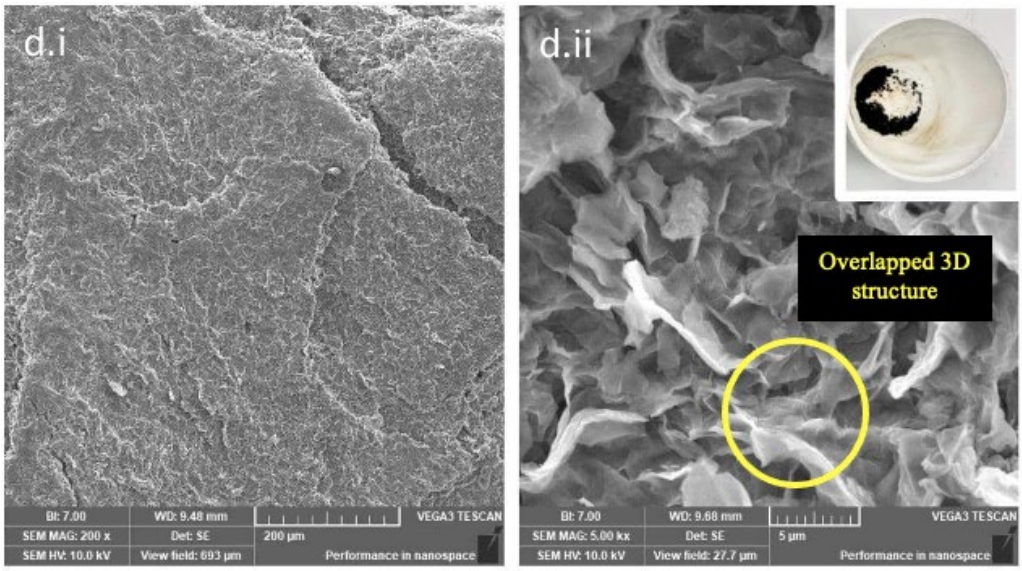

Figure 7. SEM images of rGO synthesized using banana peel extract under sonication amplitude of (a) 20 %, (b) 40 %, (c) 60 %, and (d) 80 % at 30 mins (*i.* 200x magnification and *ii.* 5000x magnification).

Further analysis showed that the rGO produced under sonication amplitude of 20 %, 40 %, 60 %, and 80 % had an interlayer spacing of 0.5 µm, 0.67 µm, 1.77 µm, and 1.93 µm, respectively (see Figure 8). Evidently, an increase in sonication amplitude induces a larger interlayer spacing of rGO as a higher sonication amplitude leads to a greater dispersion stability and deagglomeration of nanoparticles in a fluid, resulting in an enlargement in rGO interlayer spacing [23]. A pairwise t-test shows that the samples prepared under sonication amplitude of 20 % and 40 % are significantly different from the samples prepared under sonication amplitude of 60 % and 80 %, with the *p*-value being below 0.05. Thus, it is shown that the rGO produced under higher sonication amplitude of 60 % and 80 % has relatively larger interlayer spacings compared to that produced under sonication amplitude of 20 % and 40 %.

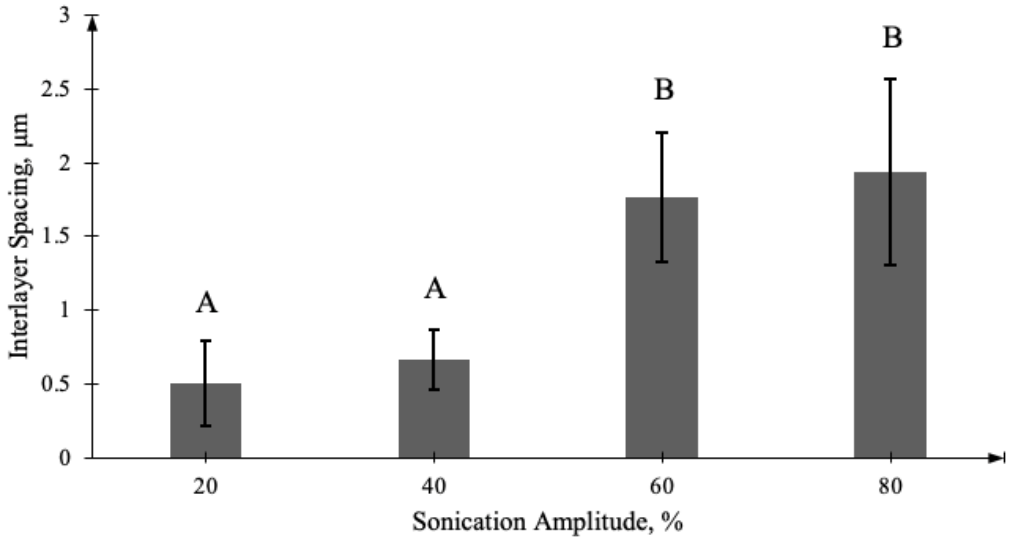

Figure 8. Interlayer spacing of rGO produced by the reduction process using banana peel extract under various sonication amplitudes at 30 mins (*Statistically significant study by t-test at $P < 0.05$).

Next, Figure 9 shows the SEM images of rGO synthesized using banana peel extract under various sonication durations. At lower magnification (200x), the produced rGO displayed a jagged and rough surface. Taking a closer look at higher magnification (5000x), the rGO shows morphology with curled edges made out of wrinkles and a few layers of paper-like texture.

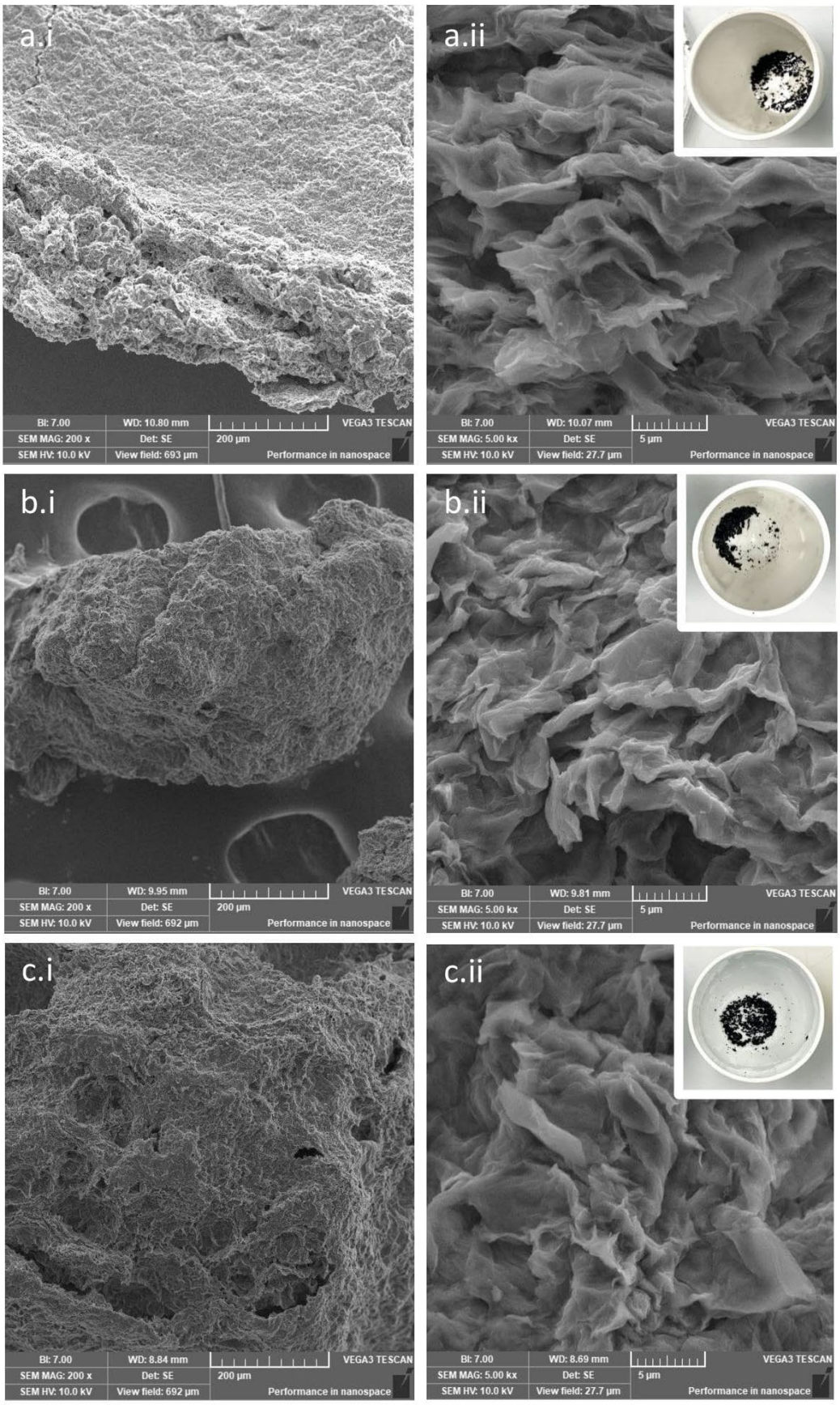
a.i
BI: 7.00
WD: 10.80 mm
VEGA3 TESCAN
SEM MAG: 200 x
Det: SE
200 µm
SEM HV: 10.0 kV
View field: 693 µm
Performance in nanospace
a.ii
BI: 7.00
WD: 10.07 mm
VEGA3 TESCAN
SEM MAG: 5.00 kx
Det: SE
5 µm
SEM HV: 10.0 kV
View field: 27.7 µm
Performance in nanospace
b.i
BI: 7.00
WD: 9.95 mm
VEGA3 TESCAN
SEM MAG: 200 x
Det: SE
200 µm
SEM HV: 10.0 kV
View field: 692 µm
Performance in nanospace
b.ii
BI: 7.00
WD: 9.81 mm
VEGA3 TESCAN
SEM MAG: 5.00 kx
Det: SE
5 µm
SEM HV: 10.0 kV
View field: 27.7 µm
Performance in nanospace
c.i
BI: 7.00
WD: 8.84 mm
VEGA3 TESCAN
SEM MAG: 200 x
Det: SE
200 µm
SEM HV: 10.0 kV
View field: 692 µm
Performance in nanospace
c.ii
BI: 7.00
WD: 8.69 mm
VEGA3 TESCAN
SEM MAG: 5.00 kx
Det: SE
5 µm
SEM HV: 10.0 kV
View field: 27.7 µm
Performance in nanospace

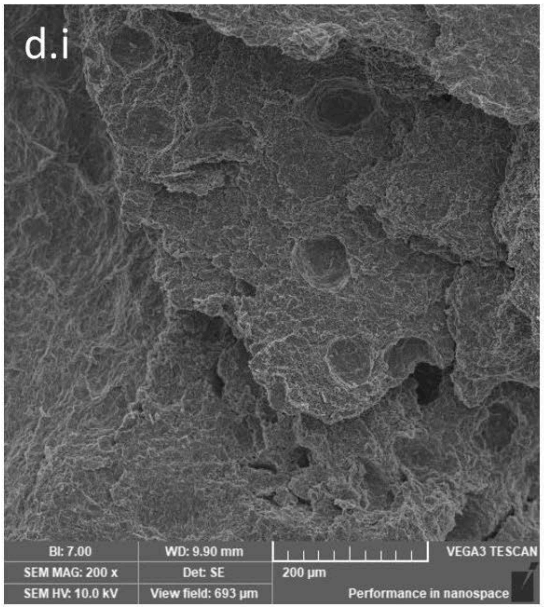
d.i
BI: 7.00
WD: 9.90 mm
VEGA3 TESCAN
SEM MAG: 200 x
Det: SE
200 µm
SEM HV: 10.0 kV
View field: 693 µm
Performance in nanospace

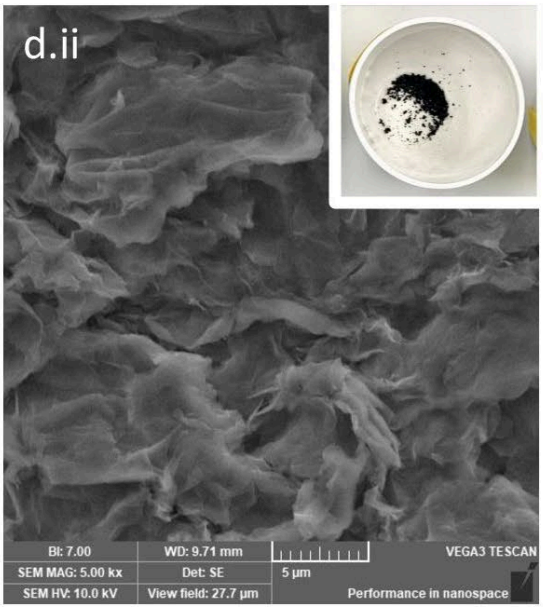
d.ii
BI: 7.00
WD: 9.71 mm
VEGA3 TESCAN
SEM MAG: 5.00 kx
Det: SE
5 µm
SEM HV: 10.0 kV
View field: 27.7 µm
Performance in nanospace

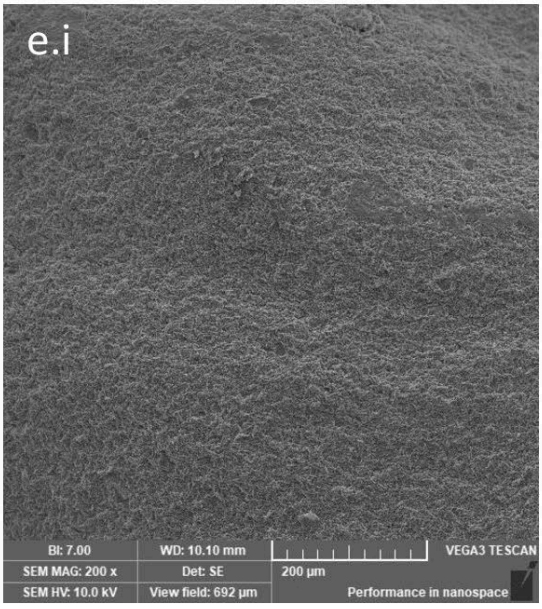
e.i
BI: 7.00
WD: 10.10 mm
VEGA3 TESCAN
SEM MAG: 200 x
Det: SE
200 µm
SEM HV: 10.0 kV
View field: 692 µm
Performance in nanospace

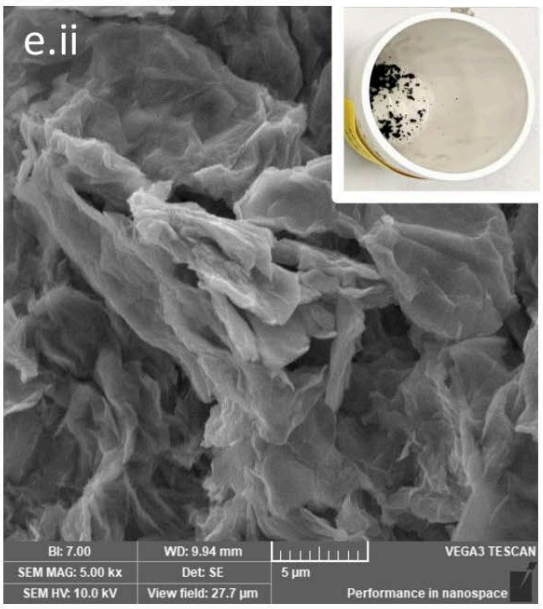
e.ii
BI: 7.00
WD: 9.94 mm
VEGA3 TESCAN
SEM MAG: 5.00 kx
Det: SE
5 µm
SEM HV: 10.0 kV
View field: 27.7 µm
Performance in nanospace

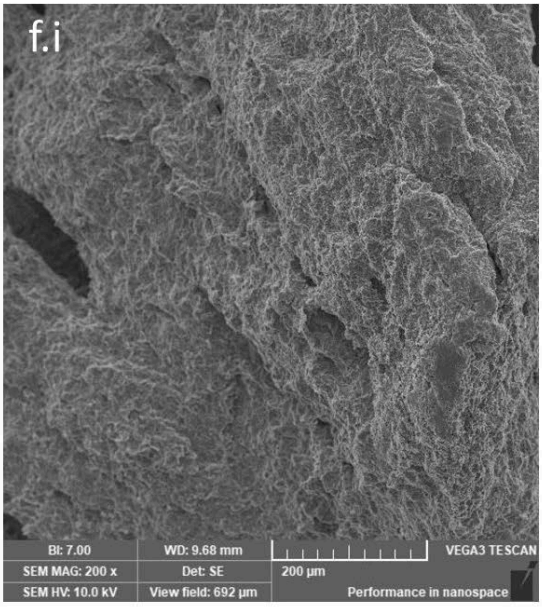
f.i
BI: 7.00
WD: 9.68 mm
VEGA3 TESCAN
SEM MAG: 200 x
Det: SE
200 µm
SEM HV: 10.0 kV
View field: 692 µm
Performance in nanospace

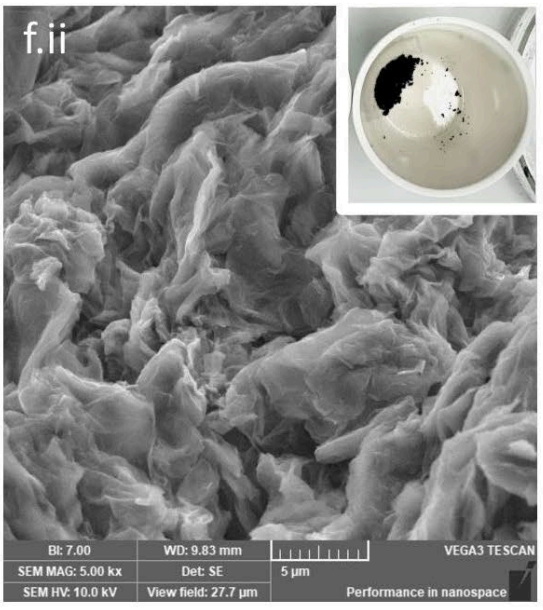
f.ii
BI: 7.00
WD: 9.83 mm
VEGA3 TESCAN
SEM MAG: 5.00 kx
Det: SE
5 µm
SEM HV: 10.0 kV
View field: 27.7 µm
Performance in nanospace

Figure 9. SEM images of rGO synthesized using banana peel extract under sonication duration of (a) 5 mins, (b) 10 mins, (c) 20 mins, (d) 30 mins, (e) 40 mins, and (f) 50 mins at 40 % amplitude (*i.* 200x magnification and *ii.* 5000x magnification).

Figure 10 delineates the interlayer spacing of rGO synthesized by banana peel extract under various sonication durations. Results showed that the rGO produced under sonication duration of 5 mins, 10 mins, 20 mins, 30 mins, 40 mins, and 50 mins has an interlayer spacing of 1.6 μm, 1.2 μm, 0.93 μm, 1 μm, 0.9 μm, and 1.13 μm, respectively. T-test analysis has shown the *p*-value to be above 0.05 for all samples, indicates that all samples are not significantly different.

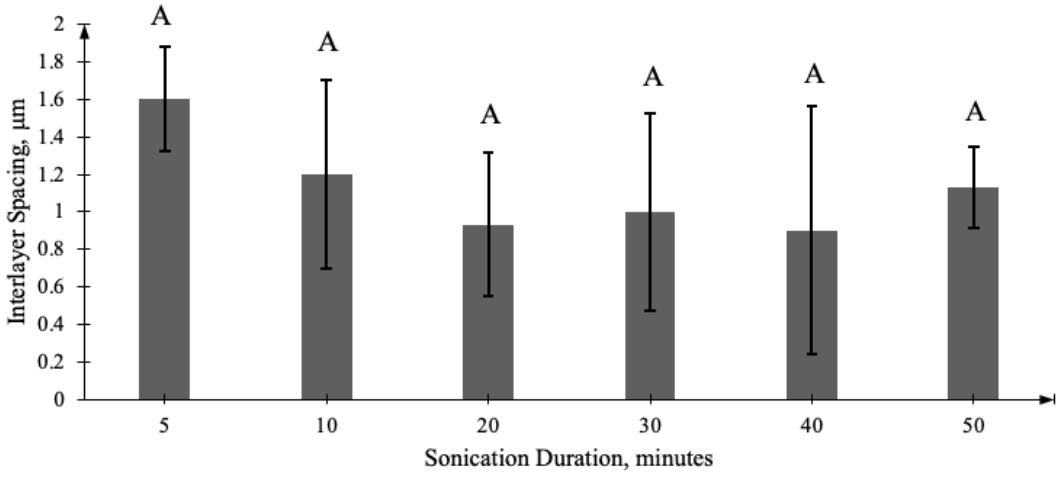

Figure 10. Interlayer spacing of rGO produced by the reduction process using banana peel extract under various sonication durations at 40 % amplitude (*Statistically significant study by t-test at $P < 0.05$).

Through visual inspection, the rGO produced using banana peel extract under stirring (Figure 5b) and under ultrasound assistance (Figures 7 and 9) exhibited similar features, such as wavy, folded, and wrinkled surfaces. Nevertheless, the interlayer spacing of the rGO sheets formed using the ultrasound approach (particularly those formed at higher sonication amplitude) is significantly greater compared to that of rGO formed under the stirring method,

further proving that the inclusion of sonication promotes a higher dispersion quality of individual nanoparticles, which widens the interlayer spacing of synthesized rGO sheets.

Surface Functional Group Analysis

FTIR Analysis of rGO Synthesized Based on Stirring

To identify the functional groups existing on the surface of rGO produced, FTIR analysis was conducted on all of the produced rGO. Figure 11 delineates FTIR spectra of rGO reduced using banana peel extract and hydrazine hydrate under 3 hours of stirring while Table 1 serves as a legend. From Figure 11, the pronounced peaks that appear on rGO reduced using banana peel extract at 1041.47 cm^{-1}, 1227.56 cm^{-1}, and 1372.38 cm^{-1} were attributed to the C-O stretching vibrations [24]. Besides, the absorption peak at 1621.22 cm^{-1} can be assigned to the C=C stretching vibrations [25]. Another peak found at 1725.46 cm^{-1} was contributed by the C=O stretching vibrations [26]. Meanwhile, the broad peak at 3174.77 cm^{-1} was attributed to the O-H stretching vibrations [24b]. On the other hand, the prominent peaks found at 1530.49 cm^{-1} on the rGO reduced using hydrazine hydrate can be attributed to the C-OH bending vibrations [24a]. Besides, the CO_2 peak that appears at 2326.12 cm^{-1} may be due to the porosity and hygroscopic nature of rGO [24b, 27].

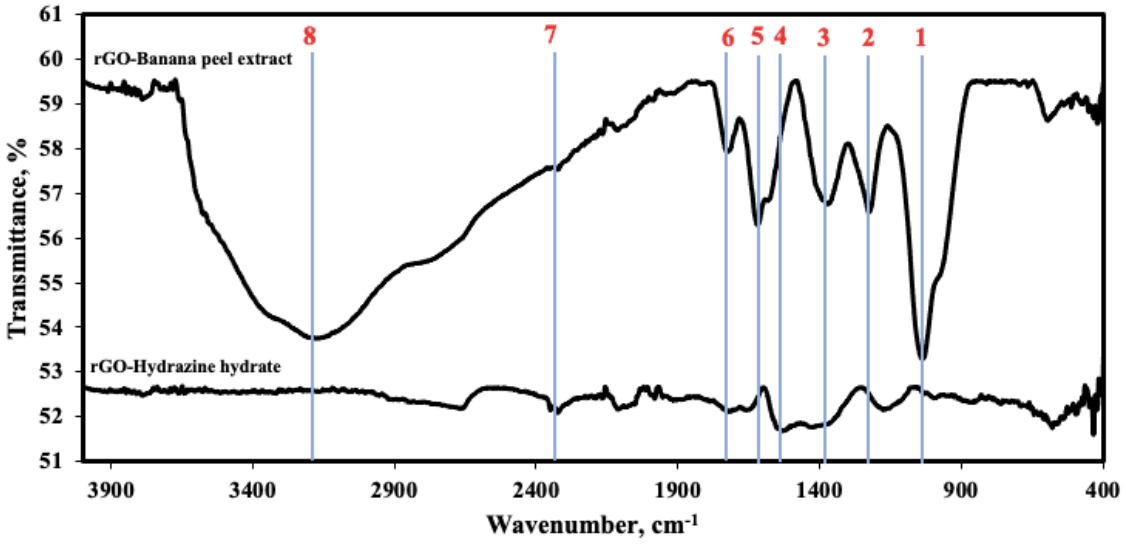

Figure 11. FTIR spectra of rGO reduced using banana peel extract, and rGO reduced using hydrazine hydrate under conventional 3 hours stirring method.

TABLE 1. Legends for FTIR spectra shown in Figure 11

No.	Wavenumber (cm^{-1})	Assignment	Reference
1	1041.47	C-O stretching vibrations	[24]
2	1227.56	C-O stretching vibrations	[24]
3	1372.39	C-O stretching vibrations	[24]
4	1530.49	C-OH bending vibrations	[24a]
5	1621.22	C=C stretching vibrations	[25]
6	1725.46	C=O stretching vibrations	[26]
7	2326.12	CO_2 peak	[24b, 27]
8	3174.77	O-H stretching vibrations	[24b]

It is noteworthy that most of the absorption peaks on the rGO reduced using banana peel extract did not appear in the spectrum of rGO reduced using hydrazine hydrate. In addition, the intensity of oxygen-functional group peaks observed on the rGO reduced using banana peel extract was only slightly lower than that on GO (see Figure S2 for FTIR of GO); this result indicates that the banana peel extract, despite being a green alternative, has a milder reducing effect than hydrazine hydrate.

FTIR Analysis of rGO Synthesized Based on Various Sonication Conditions

Subsequently, Figure 12 delineates the FTIR spectra of rGO reduced using banana peel extract under various sonication conditions. As shown in Figure 12, the rGO produced under different sonication conditions exhibited identical absorption peaks to those of rGO produced using banana peel extract under the stirring method. Overall, there is no significant difference in the intensity of FTIR spectra of the rGO produced across various sonication

amplitudes and durations. The presence of residual oxygen-functional groups indicates that the rGO was not fully reduced by the ultrasound-assisted banana peel extract reduction method.

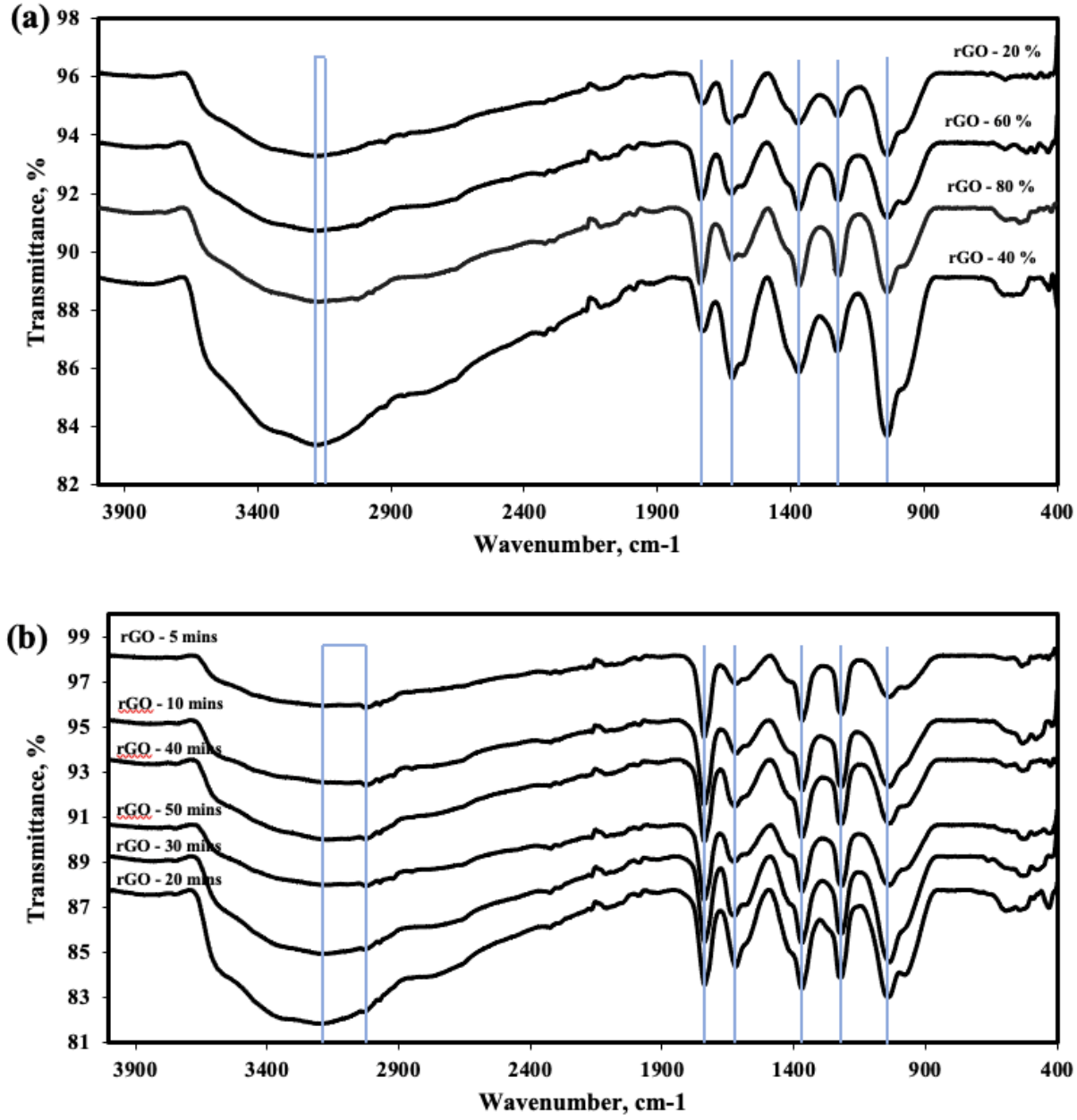

Figure 12. FTIR spectra of rGO reduced using banana peel extract under various (a) sonication amplitudes and (b) durations.

XRD Analysis for Phase Identification

Figure 13 shows the XRD profile of rGO formed using hydrazine hydrate (+ 3 hrs stirring) and that formed using banana peel extract (+ ultrasound at 20% amplitude, 30 mins). The appearance of broad peak at 2θ = ~ 30° in both samples, although close to the profile of rGO reported in literature [28], deviates from the typical (002) plane peak of rGO at 2θ = 24.5° [29]. Meanwhile, the peak at 2θ = 42.5° observed in both samples can be attributed to the (10) plane resulting from the short-range ordering of stacked graphene sheets [30]. It is worth noting that the rGO formed using hydrazine and banana peel extract presents significant peaks at 2θ = 13.17° and 2θ = 10.91°, respectively. The latter is even close to the typical peak of GO at 10.6º associated to (001) lattice plane [31]. Apparently, the rGO formed using banana peel extract retains the phase properties of GO. This observation aligns with the FTIR results, which indicates that banana peel extract acts as a weaker reducing agent compared to hydrazine.

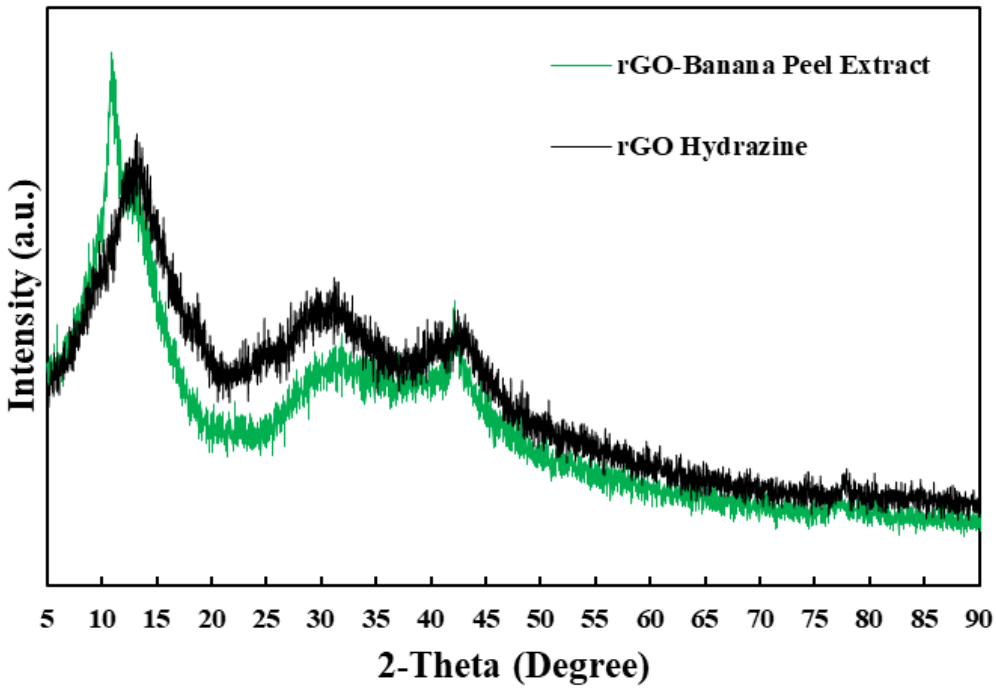

Figure 13. XRD profile of rGO reduced using banana peel extract + ultrasound (20 % amplitude, 30 mins) and hydrazine hydrate + 3 hrs stirring.

Evaluation of Electrical Properties of Synthesized rGO

Electrical Properties of rGO Synthesized Based on Stirring

The electrical conductance of filter paper, GO, and rGO was evaluated to validate that the reduction process is capable of converting non-conductive GO to conductive rGO. The electrical conductance of pure filter paper was measured as zero as the electrical resistance reached an infinite value, indicating that it is a non-conductive material (see Table 2). On the other hand, the electrical conductance of GO was measured as 2.43×10^{-6} S. GO is defined as an insulating material due to its conjugated electronic structure being broken by oxidized functional groups [32].

Table 2. Electrical resistance and electrical conductance of filter paper and GO.

Sample	Electrical Resistance	Electrical Conductance
Filter paper*	Infinity	0
GO	4.11×10^{5} Ω	2.43×10^{-6} S

*Note that the filter paper was employed as the substrate for casting GO and rGO for resistance testing. Hence, its resistance value was measured for baseline comparison.

Figure 14 shows the electrical conductance of two rGO samples produced using the conventional approach by 3 hours of stirring. Results implied that the rGO produced using hydrazine hydrate and banana peel extract (stirring) developed an electrical conductance of 5.69×10^{-6} S and 3.59×10^{-6} S, respectively. Both values are higher than that of GO, indicating that both reducing agents able to restore the electrical conductance of the graphene by removing its oxygen-containing groups. Apparently, the rGO produced by hydrazine hydrate has the highest electrical conductance, which proves that it is a well-established chemical reducing agent for the mass production of rGO. This observation aligns with FTIR spectra, which also indicate that most of the oxygen-containing groups in GO were effectively reduced using hydrazine hydrate. In comparison, the rGO produced by banana

peel extract has a slightly lower electrical conductance as it remains with some oxygen-containing groups which disrupt the conjugated electronic structure of graphene [32].

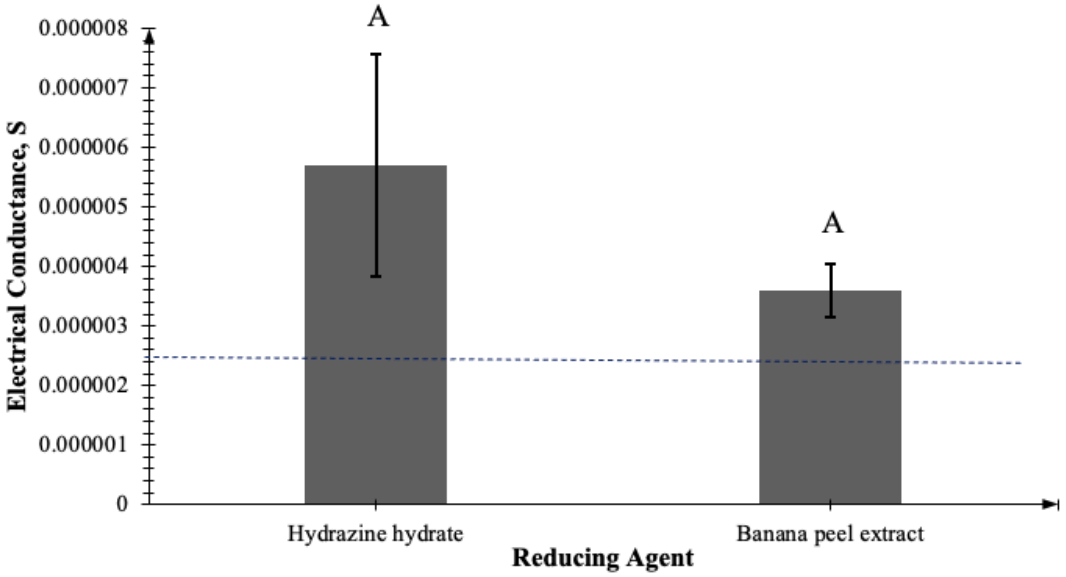

Figure 14. Electrical conductance of rGO produced by hydrazine reduction or banana peel extract reduction using 3 hours of stirring method (*Statistically significant study by t-test at $P < 0.05$). For comparison, the dashed line shows the electrical conductance of GO.

Electrical Properties of rGO Synthesized Based on Various Sonication Conditions

Next, the electrical conductance of rGO synthesized using banana peel extract upon subjected to various sonication conditions was determined in order to evaluate the role of ultrasound-assisted method compared to the conventional stirring method. As shown in Figure 15a, the rGO produced using sonication amplitude of 20 %, 40 %, 60 % and 80 % with 30 mins sonication duration exhibited electrical conductance of 4.56×10^{-6} S, 4×10^{-6} S, 3.49×10^{-6} S, and 3.74×10^{-6} S respectively. Hypothetically, an increase of ultrasonication amplitude leads to more dispersed nanofluids, a better reduction reaction and thus better restoration of electrical conductivity. However, the anticipated outcome was not significantly observed in this study. T-test analysis showed the *p*-value to be above 0.05 for all samples, indicating that all samples are not significantly different. Despite that, all of the samples

showed higher electrical conductance than GO (2.43×10^{-6} S) and comparable electrical conductance with rGO produced using banana peel extracts under the conventional stirring method (3.59×10^{-6} S).

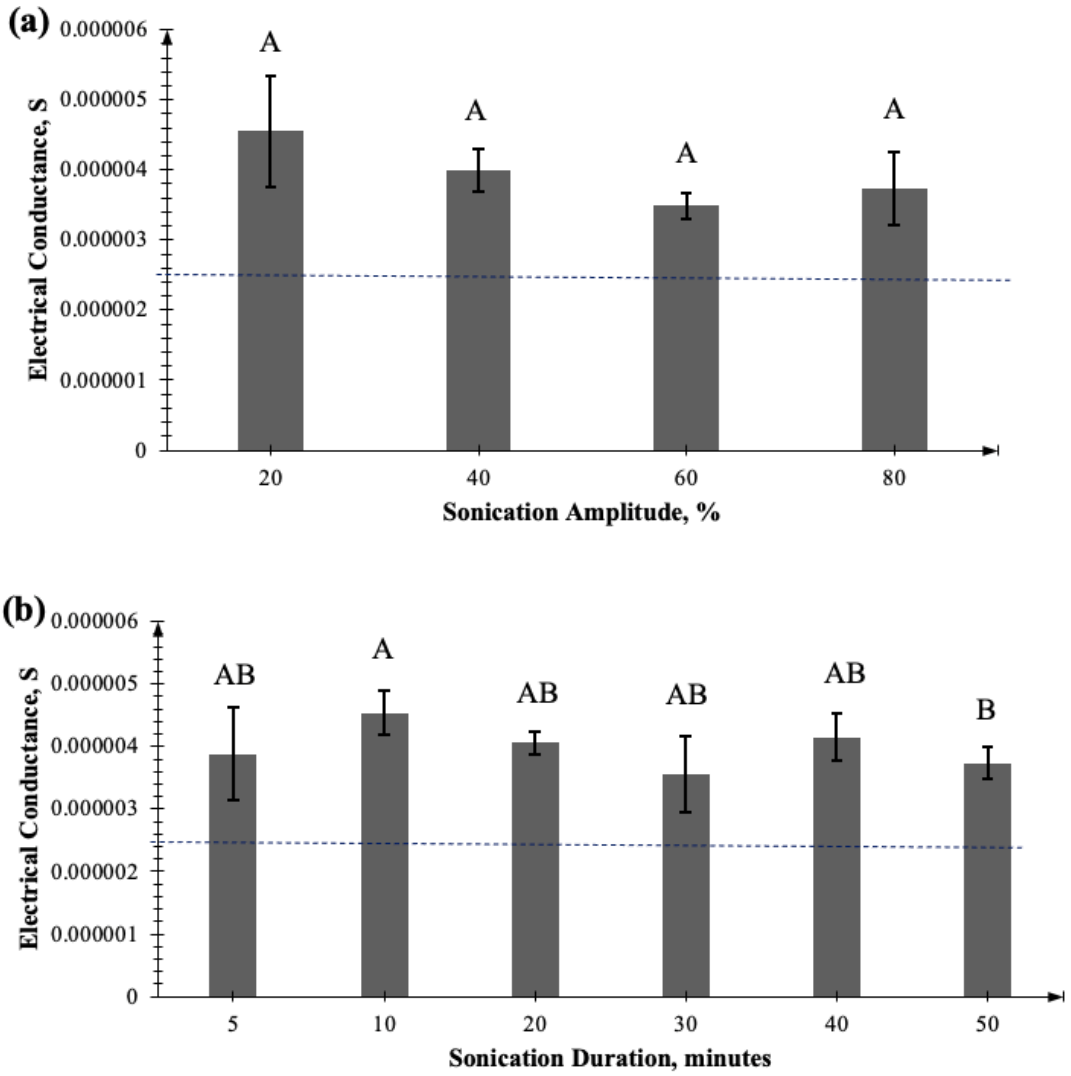

Figure 15. Electrical conductance of rGO produced by conducting the reduction process using banana peel extracts under (a) various sonication amplitudes at 30 mins sonication duration, and (b) various sonication durations at 40 % amplitude (*Statistically significant study by t-test at $P < 0.05$). For comparison, the dashed line is drawn to show the electrical conductance of GO.

Figure 15b depicts the effects induced by sonication duration. Results showed that the electrical conductance of rGO produced using sonication duration of 5 mins, 10 mins, 20 mins, 30 mins, 40 mins, and 50 mins were 3.88×10^{-6} S, 4.53×10^{-6} S, 4.06×10^{-6} S, and

3.55×10^{-6} S, 4.15×10^{-6} S, and 3.74×10^{-6} S respectively. Similarly, there is no clear trend observed across the studied sonication durations. Pairwise T-test shows that only the sample prepared under 10 mins and 50 mins are significantly different with the *p*-value below 0.05. Although the effects of sonication duration was not significantly observed, this result proves that sonication duration of 5 mins is sufficient to generate rGO with equivalent electrical conductance with those prepared under longer sonication duration or conventional stirring method. In addition to that, it was found that there is no significant relationship between the interlayer spacing of rGO layers and the electrical conductance (Figure S3).

While most of the rGO produced by banana peel extract with ultrasound assistance exhibited higher or comparable electrical conductance compared to rGO produced by banana peel extract under conventional stirring approach, this result highlights the feasibility of ultrasound techniques in rGO synthesis as an alternative to the time-consuming stirring approach.

3. Conclusion

In this study, a novel methodology was developed by assimilating green reducing agent (i.e. banana peel extract) and sonication technique into rGO synthesis. The surface morphology, functionalities, and electrical properties of the as-synthesized rGO were revealed through SEM, FTIR, XRD, and electrical conductance analyses, respectively. SEM analysis showed that the physical structures of rGO formed using banana peel extract under ultrasound technique are similar to those formed using either banana peel extract or hydrazine hydrate under conventional stirring method. Nevetheless, the rGO produced through the assistance of ultrasonication technique has a greater interlayer spacing than those formed under conventional stirring method. In particular, an increase in sonication amplitude induces a

larger rGO interlayer spacing. In terms of electrical properties, rGO produced using hydrazine hydrate was found to exhibit the highest electrical conductance of 5.69×10^{-6} S compared to those produced using banana peel extract under various ultrasound conditions (3.55×10^{-6} S - 4.56×10^{-6} S). This observation aligns with FTIR analysis, which demonstrated that hydrazine hydrate has a stronger reducing effect compared to banana peel extract, as most of the oxygen-containing functional groups were removed by hydrazine. The XRD analysis also showed that the rGO produced by banana peel extract retains the characteristics of GO due to its weak reducing effect. Despite that, results showed that most of the rGO produced by banana peel extract under ultrasound assistance has higher or comparable electrical conductance compared to the rGO produced by banana peel extract under conventional stirring method; this highlights the potential of the short period-ultrasound technique to replace conventional stirring method in rGO synthesis. The shorter duration signifies opportunities for a more efficient process that reduces operational costs, increases production, and promotes sustainable practices in industrial applications. Although banana peel extract serves as a green alternative, it possesses a milder reducing effect compared to hydrazine hydrate; further study is needed to optimize the reducing effect of the fruit peel extract so that the electrical transport properties of the graphene material can be restored to their fullest extent. In particular, several parameters including the concentration of the fruit peel extract and the temperature during reduction can be optimized.

4. Experimental Section

Preparation of Banana Peel Extract

Banana peel extract was prepared by adding 300 g of blended banana peels with 1500 mL DW in which the weight-to-volume ratio is 0.2 g/mL [6]. The mixture was then being stirred at 300 rpm for 20 mins using a magnetic stirrer. After that, the mixture was

centrifuged at 9000 rpm for 5 mins to obtain the banana peel extract (Figure S1). Subsequently, the banana peel extract was filtered using a vacuum filter to ensure there is no solid residue left in it. Lastly, the banana peel extract was stored in a beaker and kept in refrigerator prior to be used in the reducing reaction.

Preparation of Graphene Oxide (GO) via Modified Hummers' Method

GO was produced through modified Hummers' method. First, 2 g of graphite was mixed with 50 mL of sulfuric acid (H_2SO_4) in an ice bath for 10 mins. The usage of H_2SO_4 was to allow oxidizing agent to penetrate more easily into the graphene planes for graphite oxidation [33]. Following that, 6 g of potassium permanganate ($KMnO_4$) was slowly added into the solution as an oxidizing agent; the mixture was stirred at 350 rpm for a period of 40 mins. Then, 250 mL of distilled water (DW) was slowly added into the mixture, followed by 30 mL of hydrogen peroxide (H_2O_2). The mixture was stirred for 1 hour to cease the reaction and to remove excess $KMnO_4$. After that, the supernatant was removed and the GO cake was filtered using a vacuum filter. The GO was washed three times with DW. Finally, the washed GO paste was dried in an oven at 60°C for 6 days in order to produce brown-black GO flakes.

Synthesis of rGO

Ultrasound-Assisted Green Reduction Method

This study was conducted using an ultrasonic processor (Hielscher, model UP200s, 230 V/2 A/60 Hz). The effect of sonication power on rGO yield was investigated by varying the sonication power from 20 % ultrasound amplitude to 80 % ultrasound amplitude. To synthesis rGO by reduction method, 200 mg GO was dispersed in 40 mL of DW and sonicated for 3 mins to ensure a well-dispersed mixture. After that, 30 mL of banana peel extract was added into the solution as a reducing agent. The mixture was then exposed to the

ultrasound treatment with sonication power of 20 % ultrasound amplitude. On the other hand, the sonication duration was set at 30 mins with a 1 minute idle interval to avoid overheating. Subsequently, the rGO was washed with DW and filtered using a vacuum filter before being dried in an oven at 60 °C for 24 hours. The process was repeated using different sonication powers which are 40 %, 60 %, and 80 % ultrasound amplitude.

Next, the same experiment was conducted with varying sonication durations ranging from 5 mins to 50 mins, with a 1-minute idle interval to avoid overheating. At this stage, the sonication amplitude was fixed at 40 % ultrasound amplitude. Similarly, the as-synthesized rGO was washed with DW and filtered using a vacuum filter.

Conventional Stirring Method

In order to compare the quality of the produced rGO, two control rGO samples were prepared, namely rGO produced using hydrazine (without ultrasound-assisted) and banana peel extract (without ultrasound-assisted). To synthesis rGO by this reduction method, 200 mg GO was dispersed in 40 mL of DW and sonicated for 3 mins to ensure a well-dispersed mixture. After that, 30 mL of hydrazine hydrate was added into the solution as a reducing agent. Subsequently, the mixture was stirred at 350 rpm for 3 hours. The formed rGO was washed with DW and filtered using a vacuum filter. Lastly, the rGO slurry was dried in an oven at 60 °C for 24 hours. The process was repeated using banana peel extract as reducing agent. Accordingly, the role of green reducing agent and ultrasound effect can be correlated to the morphology, functionality, and electrical properties of the rGO.

Evaluation on Physicochemical Properties of the As-Synthesized rGO

Surface Morphology: Scanning Electron Microscope (SEM)

The morphology analysis of the produced rGO was viewed using SEM (Tescan VEGA3 with platinum coating). The completely dried rGO powder was carefully placed on a sticky tape before being placed on the SEM holder. The three-dimensional surface morphology of rGO was then captured at an accelerated voltage of 10 kV at different magnifications.

Surface Functionalities: Fourier Transform-Infrared Spectrometry (FT-IR)

The presence and absence of oxygen-functional groups of GO and rGO was investigated using FT-IR (Perkin Elmer (Spectrum Two)). The GO and rGO samples were scanned in the wavenumber range from 400 cm^{-1} to 4000 cm^{-1} in order to obtain the FT-IR spectra for further comparison. Similarly, FT-IR analysis was conducted for rGO produced under green and hydrazine reduction method as to evaluate the effect of green reduction on surface functionalities of the produced rGO.

Phase Identification: X-ray Diffraction (XRD)

The phase properties of the rGO formed using a conventional reducing agent and the ultrasound-assisted green reduction method were determined via XRD analysis (Bruker D8 Discover). The powder XRD analysis was carried out using Cu Kα radiation ((k = 1.5418 Å) operated at accelerating voltage 40 kV and emission current 40 mA. The XRD profile scan was performed over a 2θ range from 5° to 90° with a step size of 0.021° at room temperature (25°C).

Electrical Properties: Two-Point Probe Method

The electrical conductivity of rGO produced through green reduction method under various sonication conditions were determined and be compared to rGO which is reduced using conventional reducing agent (i.e. hydrazine). Here, the rGO were coated onto filter papers using PVA glue; then, the rGO-coated filter paper was connected to a multimeter set at 20 kΩ for resistance measurement [34]. Three measurements were conducted for each sample in order to obtain an average value.

Significance Analysis: Pairwise T-Test

The significance analysis of the interlayer spacing and electrical conductance of rGO produced using conventional stirring and sonication methods, with both conventional and green reducing agents, was conducted through pairwise t-tests, respectively. This analysis aimed to compare the means of two independent groups to determine if they are significantly different. The average values and standard deviations of the interlayer spacing and electrical conductance of rGO were used to calculate the error bars for each sample, enabling the determination of *p*-values and specific comparisons between the datasets.

Credit Authorship Contribution Statement

Shuen Lam: Methodology, Formal analysis, Investigation, Writing - Original Draft. **Fei Wang**: Methodology, Investigation. **Swee Pin Yeap**: Conceptualization, Visualization, Supervision, Resources, Funding acquisition, Validation, Writing - Review & Editing. **Kah Hou Teng**: Conceptualization, Resources, Writing - Review & Editing. **Andy Shaw**: Conceptualization, Supervision. **Vijayakumar Karunamoothei**: Visualization, Project administration, Resources. **Vahid Khosravi**: Methodology, Project administration**. Chengyi Liu**: Supervision, Project administration, Resources.

Data Availability

Data available on request from the authors.

Conflict of interest

There are no conflicts to declare.

Acknowledgement

This project is funded by the Ministry of Higher Education Malaysia through Fundamental Research Grant Scheme (FRGS) with project code FRGS/1/2020/TK0/UCSI/03/3.

Keywords

Electrical Properties; Fruit Extract; Graphene; Green Synthesis; Ultrasound Technique

References

[1] aS. H. Alwan, A. A. Omran, D. K. Naser, M. F. Ramadan, *Engineering Proceedings* **2023**, *59*, 226; bA. R. Urade, I. Lahiri, K. S. Suresh, *JOM* **2023**, *75*, 614-630.

[2] C. Buelke, A. Alshami, J. Casler, J. Lewis, M. Al-Sayaghi, M. A. Hickner, *Desalination* **2018**, *448*, 113-132.

[3] aA. T. Smith, A. M. LaChance, S. Zeng, B. Liu, L. Sun, *Nano Materials Science* **2019**, *1*, 31-47; bM. Chitkara, N. Goyal, A. Kumar, L. Marasamy, S. Haq, S. A. Aldossari, R. Haldhar, M. K. Hossain, *RSC Advances* **2024**, *14*, 8769-8778.

[4] aC. E. Jee, M. K. Chow, S. P. Yeap, *Journal of Applied Polymer Science* **2023**, *140*, e53415; bY. Sun, Z. Zhang, C. Xiang, Y. Jiang, Y. Feng, X. Cheng, X. Li, M. Wang, *CrystEngComm* **2024**.

[5] aR. Wijaya, G. Andersan, S. Permatasari Santoso, W. Irawaty, *Scientific Reports* **2020**, *10*, 667; bS. J. An, Y. Zhu, S. H. Lee, M. D. Stoller, T. Emilsson, S. Park, A. Velamakanni, J. An, R. S. Ruoff, *The Journal of Physical Chemistry Letters* **2010**, *1*, 1259-1263.

[6] L. Buasuwan, V. Niyomnaitham, A. Tandaechanurat, *MRS Advances* **2019**, *4*, 2143-2151.

[7] aA. M. Amani, L. Tayebi, E. Vafa, M. Abbasi, A. Vaez, H. Kamyab, S. Chelliapan, M. J. Azizli, R. Bazargan-Lari, *Journal of Cleaner Production* **2024**, *436*, 140606; bJ. A. Kumar, T. Krithiga, S. Manigandan, S. Sathish, A. A. Renita, P. Prakash, B. S. N.

Prasad, T. R. P. Kumar, M. Rajasimman, A. Hosseini-Bandegharaei, D. Prabu, S. Crispin, *Journal of Cleaner Production* **2021**, *324*, 129198.
[8] R. Joshi, A. De Adhikari, A. Dey, I. Lahiri, *Materials Science and Engineering: B* **2023**, *287*, 116128.
[9] A. E. D. Mahmoud, M. Hosny, N. El-Maghrabi, M. Fawzy, *Sustainable Environment Research* **2022**, *32*, 22.
[10] H. A. Abdulmageed, A. K. Judran, F. T. M. Noori, *Journal of Physics: Conference Series* **2021**, *1795*, 012070.
[11] V. Priliana, C. Sucitro, R. Wijaya, V. B. Lunardi, S. P. Santoso, M. Yuliana, C. Gunarto, A. E. Angkawijaya, W. Irawaty, *Sustainability* **2022**, *14*, 12172.
[12] aH. Liu, S. Wang, L. Fu, G. Zhang, Y. Zuo, L. Zhang, *Journal of Cleaner Production* **2022**, *379*, 134775; bD. Schieppati, A. Dreux, W. Gao, P. Fatehi, D. C. Boffito, *Journal of Cleaner Production* **2022**, *366*, 132776.
[13] A. Vartolomei, I. Calinescu, M. Vinatoru, A. I. Gavrila, *Scientific Reports* **2022**, *12*, 1421.
[14] J. H. Warner, F. Schäffel, A. Bachmatiuk, M. H. Rümmeli, in *Graphene* (Eds.: J. H. Warner, F. Schäffel, A. Bachmatiuk, M. H. Rümmeli), Elsevier, **2013**, pp. 129-228.
[15] aW. M. Hikal, H. A. H. Said-Al Ahl, A. Bratovcic, K. G. Tkachenko, J. Sharifi-Rad, M. Kačániová, M. Elhourri, M. Atanassova, *Evidence-Based Complementary and Alternative Medicine* **2022**, *2022*, 7616452; bR. González-Montelongo, M. Gloria Lobo, M. González, *Food Chemistry* **2010**, *119*, 1030-1039; cP. Saravana Kumari, R. Ranjitha, N. Vidhya, *Annals of Phytomedicine* **2020**, *9*, 215-222.
[16] aM. R. Islam, M. M. Kamal, M. R. Kabir, M. M. Hasan, A. R. Haque, S. M. K. Hasan, *Measurement: Food* **2023**, *10*, 100085; bV. Balajee, S. Lokesh Kumar, S. Rajesh Kumar, *Cureus* **2023**, *15*, e51260.
[17] M. Kashif, E. Jaafar, P. Bhadja, F. Wah Low, S. Kudnie Sahari, S. Hussain, F. Kai Loong, A. Ahmad, T. Saad AlGarni, M. Shafa, H. Asghar, S. A. Al-Tamrah, *Arabian Journal of Chemistry* **2021**, *14*, 102953.
[18] aR. Hack, C. H. G. Correia, R. A. D. S. Zanon, S. H. Pezzin, *Revista Matéria* **2018**, *23*; bM. K. Chow, C. E. Jee, S. P. Yeap, *Results in Engineering* **2022**, *16*, 100682.
[19] V. B. Mohan, R. Brown, K. Jayaraman, D. Bhattacharyya, *Materials Science and Engineering: B* **2015**, *193*, 49-60.
[20] T. Ludwig, M. Je, H. Choi, T. Fischer, S. Roitsch, R. Müller, R. S. Mane, K. H. Kim, S. Mathur, *Nano Energy* **2020**, *78*, 105286.
[21] A. Alhadhrami, S. Salgado, V. Maheshwari, *RSC Advances* **2016**, *6*, 70012-70017.
[22] Z.-l. Wang, D. Xu, Y. Huang, Z. Wu, L.-m. Wang, X.-b. Zhang, *Chemical Communications* **2012**, *48*, 976-978.
[23] A. Asadi, F. Pourfattah, I. Miklós Szilágyi, M. Afrand, G. Żyła, H. Seon Ahn, S. Wongwises, H. Minh Nguyen, A. Arabkoohsar, O. Mahian, *Ultrasonics Sonochemistry* **2019**, *58*, 104701.
[24] aE. Andrijanto, S. Shoelarta, G. Subiyanto, S. Rifki, *AIP Conference Proceedings* **2016**, *1725*; bSudesh, N. Kumar, S. Das, C. Bernhard, G. D. Varma, *Superconductor Science and Technology* **2013**, *26*, 095008.
[25] R. A. Rochman, S. Wahyuningsih, A. H. Ramelan, Q. A. Hanif, *IOP Conference Series: Materials Science and Engineering* **2019**, *509*, 012119.
[26] N. J. Panicker, J. Das, P. P. Sahu, *Materials Today: Proceedings* **2021**, *46*, 6270-6274.
[27] I. O. Faniyi, O. Fasakin, B. Olofinjana, A. S. Adekunle, T. V. Oluwasusi, M. A. Eleruja, E. O. B. Ajayi, *SN Applied Sciences* **2019**, *1*, 1181.
[28] aK. Sa, P. C. Mahakul, B. V. R. S. Subramanyam, J. Raiguru, S. Das, I. Alam, P. Mahanandia, *IOP Conference Series: Materials Science and Engineering* **2018**, *338*,

012055; bJ. Y. Tee, F. L. Ng, F. S. Keng, C. W. Lee, B. Zhang, S. Lin, G. Gnana Kumar, S. M. Phang, *iScience* **2024**, *27*, 109564.
[29] H.-J. Kim, D.-E. Kim, *Scientific Reports* **2015**, *5*, 17034.
[30] aL. Stobinski, B. Lesiak, A. Malolepszy, M. Mazurkiewicz, B. Mierzwa, J. Zemek, P. Jiricek, I. Bieloshapka, *Journal of Electron Spectroscopy and Related Phenomena* **2014**, *195*, 145-154; bA. B. Rahaman, A. Sarkar, T. Singha, K. Chakraborty, S. Dutta, T. Pal, S. Ghosh, P. K. Datta, D. Banerjee, *Nanoscale Advances* **2020**, *2*, 1573-1582.
[31] A. M. Golsheikh, N. M. Huang, H. N. Lim, R. Zakaria, *RSC Advances* **2014**, *4*, 36401-36411.
[32] P. Majumder, R. Gangopadhyay, *RSC Advances* **2022**, *12*, 5686-5719.
[33] Y.-p. Chen, S.-y. Li, R.-y. Luo, X.-m. Lv, X.-j. Wang, *New Carbon Materials* **2013**, *28*, 435-441.
[34] aM. K. H. Ko Ko, S. P. Yeap, A. H. Abu Bakar, *Journal of the Taiwan Institute of Chemical Engineers* **2023**, *144*, 104735; bW. S. Koh, L. F. Khaw, S. P. Yeap, K. M. Lee, J. Y. Sum, P. Y. Toh, *Polym. Int.* **2023**, *72*, 558-568.

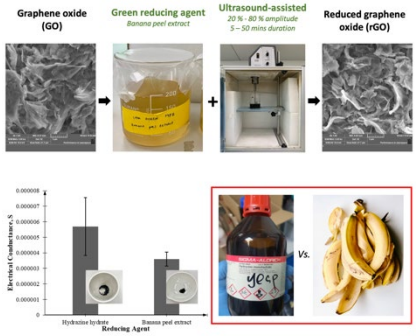

Conventional methods for synthesizing rGO often involve toxic reducing agents, posing significant environmental and health risks. This study demonstrates that the ultrasound-assisted reduction approach using banana peel extract is a viable method for synthesizing rGO. The properties of the produced rGO are compared to those of rGO produced using conventional reducing agents with stirring.